Improving Lunar Return Entry Footprints Using Enhanced Skip Trajectory Guidance

Z. R. Putnam* and R. D. Braun†
Georgia Institute of Technology, Atlanta, GA, 30332

and

S. H. Bairstow‡ and G. H. Barton§
Charles Stark Draper Laboratory, Cambridge, MA, 02139

The impending development of NASA's Crew Exploration Vehicle (CEV) will require a new entry guidance algorithm that provides sufficient performance to meet all requirements. This study examined the effects on entry footprints of enhancing the skip trajectory entry guidance used in the Apollo program. The skip trajectory entry guidance was modified to include a numerical predictor-corrector phase during atmospheric skip portion of the entry trajectory. Four degree-of-freedom simulation was used to determine the footprint of the entry vehicle for the baseline Apollo entry guidance and predictor-corrector enhanced guidance with both high and low lofting at several lunar return entry conditions. The results show that the predictor-corrector guidance modification significantly improves the entry footprint of the CEV for the lunar return mission. The performance provided by the enhanced algorithm is likely to meet the entry range requirements for the CEV.

Nomenclature

L/D = lift-to-drag ratio, nondimensional

I. Introduction

In 2004, the President of the United States fundamentally shifted the priorities of America's civil space program with the Vision for Space Exploration (VSE), calling for long term human exploration of the Moon, Mars and beyond.[1] This program focuses on returning astronauts to the Moon by 2020 with the eventual establishment of a permanent manned station there. Experience gained from human exploration of the Moon is then to be used to prepare for a human mission to Mars. To complete these tasks, a new human exploration vehicle, the Crew Exploration Vehicle (CEV) will be developed.

The NASA Exploration Systems Architecture Study (ESAS) selected a CEV similar to the Apollo program's Command and Service Module, with a crewed command module and uncrewed service module.[2] The CEV command module will be a scaled version of the Apollo Command Module (CM), maintaining the same outer moldline with a larger radius. In addition, the CEV will be required to return safely to land locations during normal operations, as opposed to the ocean landings performed in the Apollo program. Successful land recovery operations require an entry guidance algorithm capable of providing accurate landings over a large capability footprint. Preliminary requirements indicate that the CEV entry vehicle must be capable of downranges of at least 10000 km.[3]

The Apollo program entry guidance contained a long range option to provide an abort mode in the event of poor weather conditions at the primary landing site. A long range entry capability also simplifies the phasing and targeting problem by allowing the vehicle to perform entry targeting within the atmosphere during entry, possibly saving propellant during in-space entry targeting. Long range entries can be easily achieved by moderate L/D blunt body entry vehicles, such as the CEV, by employing a skipping entry trajectory. When performing a skipping entry,

* Graduate Research Assistant, School of Aerospace Engineering, 270 Ferst Drive, AIAA Student Member.
† Associate Professor, School of Aerospace Engineering, 270 Ferst Drive, AIAA Associate Fellow.
‡ Draper Fellow, Mission Design and Analysis, 555 Technology Sq., AIAA Member.
§ Group Leader, Mission Design and Analysis, 555 Technology Sq., AIAA Member.

the vehicle enters the atmosphere and begins to decelerate. The vehicle then uses aerodynamic forces to execute a pull-up maneuver, lofting the vehicle to higher altitudes, possibly exiting the atmosphere. However, enough energy is dissipated during the first atmospheric flight segment to ensure that the vehicle will enter the atmosphere a second time, at a point significantly farther downrange than the initial entry point. After the second entry, the vehicle proceeds to the surface. A longer range trajectory is achieved in this manner, shown in Fig. 1.

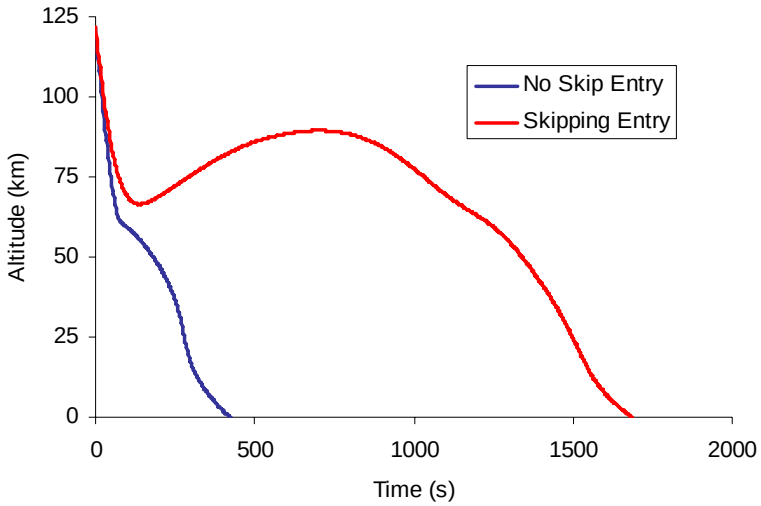

Fig. 1 Skipping and Non-skipping Entry Trajectories (Altitude vs Time).

The Apollo CM was capable of a maximum entry downrange without dispersions of 4630 km (2500 nmi) when employing the Kepler (ballistic) phase of its skip trajectory guidance.[4] However, this capability was never utilized. Studies for the First Lunar Outpost in the early 1990s used a 1.05 scale Apollo CM. These studies also employed the Apollo entry guidance algorithm, and found a similar maximum downrange without dispersions of 4445 km (2400 nmi).[5] However, in this study, trajectories using the Kepler phase of the guidance were excluded from nominal trajectory design for the following reasons:

1) Desire to maintain aerodynamic control of the vehicle throughout entry
2) Relative difficulty of accurate manual control to long range targets in the event of a guidance failure
3) Sensitivity to uncertainty at atmospheric interface and within the atmosphere leading to inaccurate landings
4) No operational necessity for long range entries[5]

While these issues remain significant concerns for the design of the CEV entry system, preliminary requirements state that the CEV must be able to achieve a downrange of at least 10000 km. Recent analyses indicate that the moldline of the CEV is fully capable of achieving downranges of this magnitude.[6] However, significant enhancements in the Apollo algorithm are required to maintain landed accuracy at these downranges.

II. Method

The entry footprint of the CEV entry vehicle was evaluated with a four degree-of-freedom simulation written in Matlab and Simulink. Entry trajectories were simulated over a range of flight path angles, crossrange and downrange commands using the baseline Apollo skip trajectory guidance and both high and low lofting predictor-corrector enhanced entry guidance algorithms. Uncertainty analysis was not included in this feasibility study.

A. Definitions

This study utilized the following definitions. Atmospheric interface, the altitude at which the entry vehicle enters the sensible atmosphere, was defined to be 122 km (400,000 ft) above the Earth's reference ellipsoid. Flight path angle (FPA) refers to the entry vehicle's inertial flight path angle at atmospheric interface. The inertial flight path angle is the angle between the vehicle's velocity vector and the local horizontal, where negative values refer to angles below the horizon. Downrange is defined to be the in-plane distance traveled by the vehicle from atmospheric interface to landing. Crossrange is defined to be the out-of-plane distance traveled by the vehicle from atmospheric

interface to landing. Miss distance is defined as the distance between the targeted landing site and the actual landing site. For the purposes of this study, an acceptable footprint was defined to be the region within which the CM achieved a miss distance of 3.5 km or less.

B. Assumptions

Several assumptions were made for the analysis performed in this study. The atmosphere was assumed to be the 1962 U.S. Standard Atmosphere to facilitate comparison with original Apollo program data. All entries were assumed to be posigrade equatorial. The entry state used is given in Table 1. The entry vehicle used was a scaled Apollo CM, as outlined in the ESAS,[2] with a maximum diameter of 5 m. Hypersonic blunt body aerodynamics were used, and the vehicle was flown at trim angle of attack, generating a lift-to-drag ratio (L/D) of 0.4. Entry vehicle properties are summarized in Table 2.

Table 1. Vehicle Entry State.

Parameter	Value
Inertial Velocity	11032 m/s
Altitude	122 km
Longitude	0 deg
Latitude	0 deg
Azimuth	90 deg

Table 2. Vehicle Properties.

Parameter	Value
Mass	8075 kg
Reference Area	23.758 m^2
L/D	0.4

C. Parameters Varied

Crossrange commands were varied between 0 km and 1000 km; downrange commands were varied between 1500 km and 13000 km. This set of commands fully captured the capability footprint of the entry vehicle. Three flight path angles were selected to examine vehicle footprints over a range of atmospheric interface conditions, as shown in the Table 3. Two of the FPAs were selected based on a CEV emergency ballistic entry (EBE) study conducted at the Charles Stark Draper Laboratory in September 2005. This set of parameters was used with both the baseline skip trajectory guidance and the high and low lofting versions of the enhanced skip trajectory guidance.

Table 3. Flight Path Angle Selections.

FPA	Selection Criteria
-5.635 deg	Center of aerodynamic corridor
-5.900 deg	Approximate shallow boundary for EBE
-6.100 deg	Approximate steep boundary for EBE

III. Results: Baseline Algorithm

A. Baseline Algorithm Description

The primary function of the entry guidance algorithm is to manage energy as the spacecraft descends to the parachute deploy interface. The bank-to-steer algorithm controls lift in the coupled vertical and lateral channels, with guidance cycles occurring at a frequency of 0.5 Hz.

Guidance's chief goal is to manage lift in the vertical channel so that the vehicle enters into the wind-corrected parachute deploy box at the appropriate downrange position. For a given FPA, full lift-up provides maximum range

while full lift-down provides the steepest descent. Lift-down may be constrained by the maximum allowed g-loads that can be experienced by the crew and vehicle. Any bank orientation other than full lift-up or full lift-down will result in a component of lift in the lateral channel. Crossrange position is controlled in the lateral channel by reversing the lift command into the mirror quadrant (e.g. +30 deg from vertical to -30 deg) once the lateral range errors to the target cross a threshold. The vehicle continues this bank command reversal strategy as it descends to the target. As the energy and velocity decrease, the lateral threshold is reduced so that the vehicle maintains control authority to minimize the lateral errors prior to chute deploy.

The baseline Apollo algorithm consists of seven phases designed to control the downrange position of the vehicle, as shown in Fig. 2.

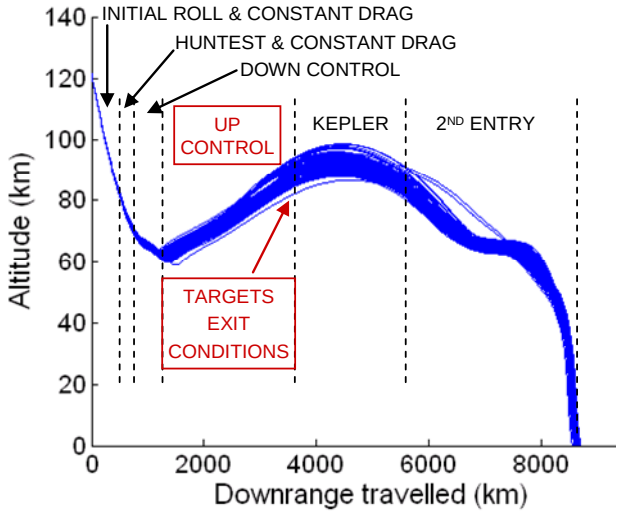

Fig. 2 Baseline Algorithm Entry Guidance Phases.

1) Pre-entry Attitude Hold: maintains current attitude until a sensible atmosphere has been detected.
2) Initial Roll: seeks to guide the vehicle toward the center of the entry corridor, nominally commanding the lift vector upward, otherwise commanding the lift vector downward to steepen a shallow entry.
3) Huntest and Constant Drag: begins once atmospheric capture is assured, triggered by an altitude rate threshold. This phase determines whether the vehicle will need to perform an upward "skip" in order to extend the vehicle's range, decides which of the possible phases to use, and calculates the conditions which will trigger those phases. The algorithm transitions to the Downcontrol phase once a suitable skip trajectory is calculated; otherwise the algorithm transitions directly to the Final ("Second Entry") phase if no skip is needed.
4) Downcontrol: guides the vehicle to pullout using a constant drag policy.
5) Upcontrol: guides the vehicle along a reference trajectory, previously generated by the Huntest phase. This trajectory is not updated during the Upcontrol phase. The algorithm transitions into the Kepler phase if the skip trajectory is large enough to exit the atmosphere; otherwise, the algorithm transitions directly into the Final ("Second Entry") phase.
6) Kepler ("Ballistic"): maintains current attitude along the velocity vector from atmospheric exit to atmospheric second entry. Exit and second entry transitions are defined to occur at an aerodynamic acceleration of 0.2 g's.
7) Final ("Second Entry"): guides the vehicle along a stored nominal reference trajectory, calculated preflight. Once the velocity drops below a threshold value, the algorithm stops updating bank commands and the guidance algorithm is disabled.

The guidance phases and phase-transition logic are discussed fully in Reference 7.

B. Results Summary

The results presented below are given in footprint plots. These plots show the miss distance associated with a particular downrange and crossrange command. Dark blue areas indicate accurate landings, while red areas indicate large miss distances. Light blue and dark blue areas provide acceptable accuracy, corresponding to miss distances of

3.5 km or less. It should be noted that red areas denote miss distance of 10 km or greater, with some miss distances in excess of 1000 km.

C. Baseline Algorithm Results

The entry guidance algorithm used for the Apollo program was selected as the baseline algorithm for the CM entry guidance. Figures 1-3 below show the landed accuracy over a range of downrange and crossrange commands for several FPAs (see Table 3). Figure 4 shows the footprint outlines at several FPAs.

Fig. 3 shows the footprint for the baseline algorithm at a FPA of -5.635 deg. Maximum crossrange is approximately ±700 km. Minimum downrange is 2250 km; maximum downrange is 7000 km. Within these ranges, the algorithm performs well. Fig. 4 shows the footprint for the baseline algorithm at a FPA of -5.900 deg. Performance remains similar at this FPA. The minimum downrange decreases to 2000 km, while the maximum downrange remains 7000 km, with the exception of crossranges less than ±50 km. Some improvement is made in long range performance, but accurate regions are patchy. Fig. 5 shows the footprint for the baseline algorithm at a FPA of -6.100 deg. Significant performance improvements are visible at this FPA. Maximum downrange increases to 7500 km; minimum downrange is 2000 km. Maximum crossrange increases to ±750 km at large downranges. Long range performance becomes accurate in two regions at crossranges greater than 400 km.

Overall, the baseline algorithm provides good performance over downrange commands between 2000 km and 7000 km with crossranges up to 700 km, as shown in Fig. 6. However, improvement is required for long range performance.

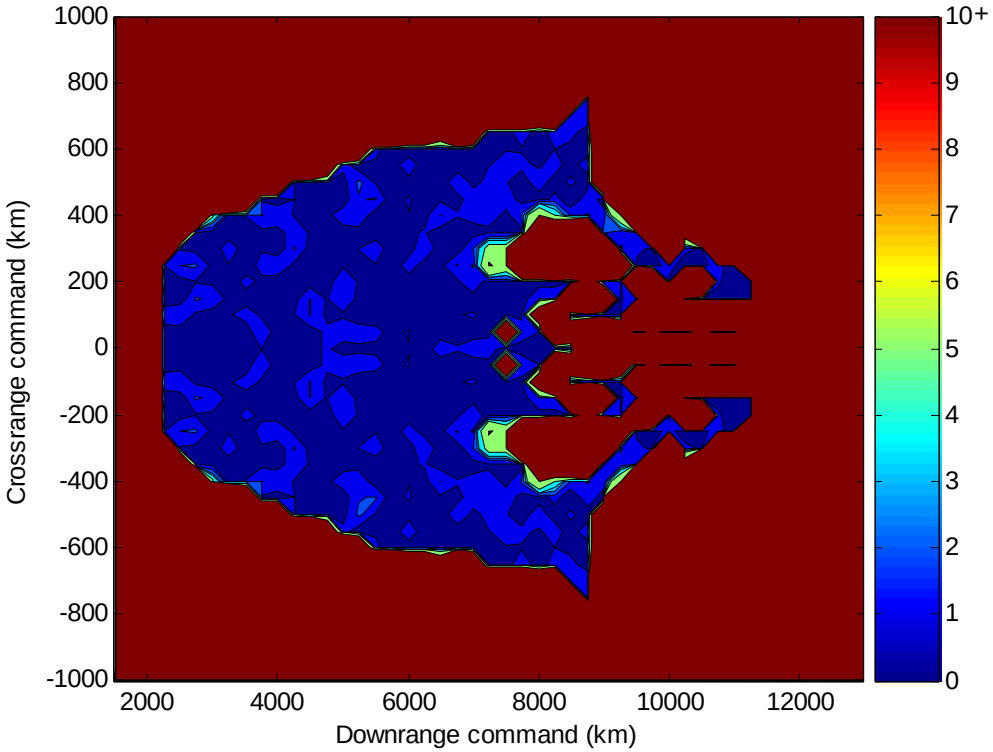

Fig. 3 Baseline miss distance (km) with FPA = -5.635 deg.

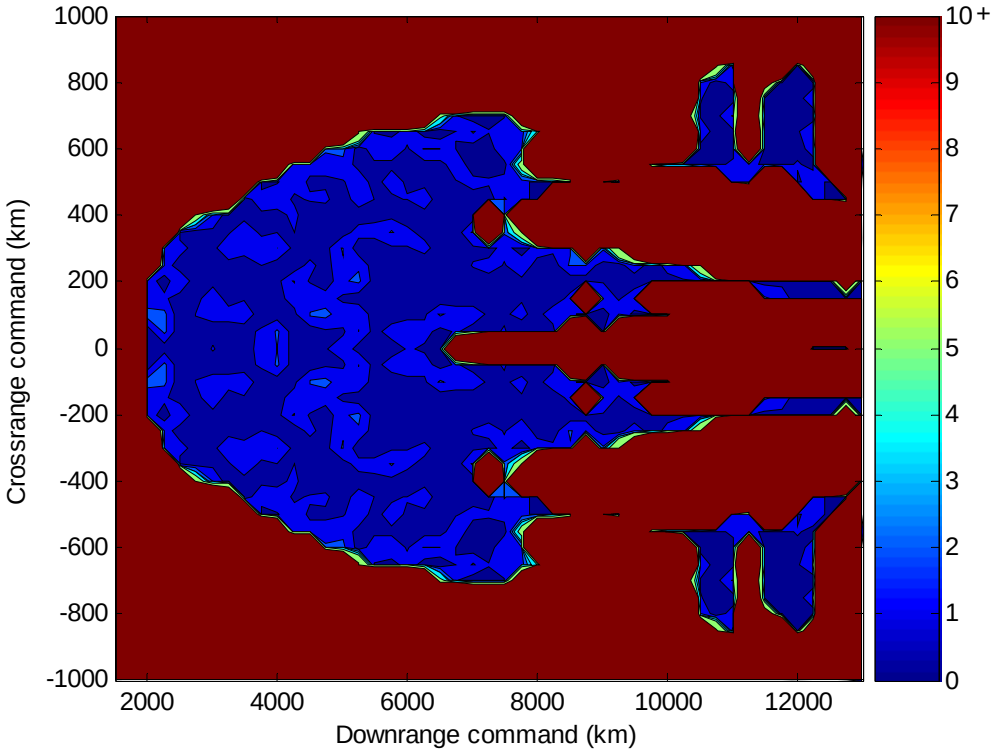

Fig. 4 Baseline miss distance (km) with FPA = -5.900 deg.

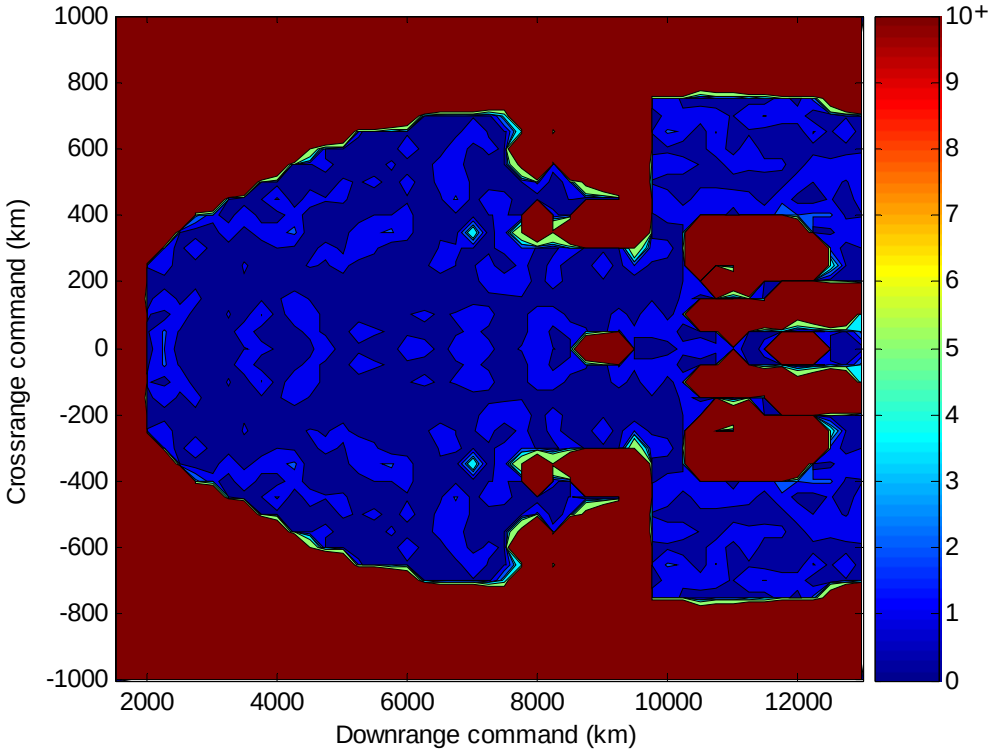

Fig. 5 Baseline miss distance (km) with FPA = -6.100 deg.

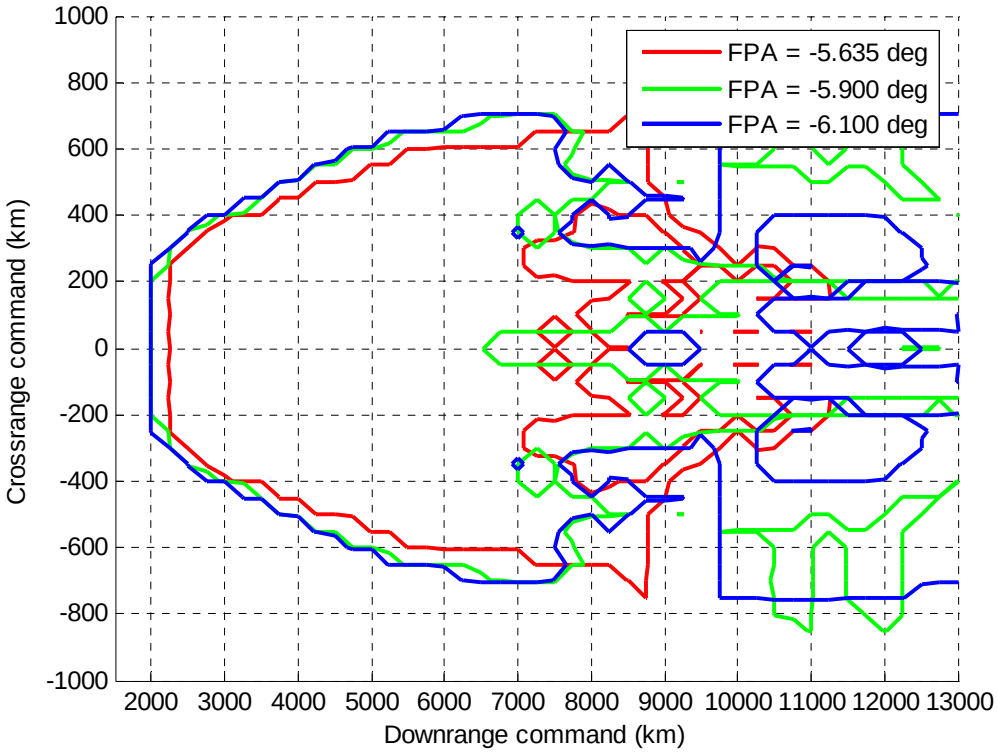

Fig. 6 Baseline range capability over several FPAs, miss distance < 3.5 km.

D. Rationale for Algorithm Improvement

Analysis of trajectories for long target ranges showed that the degradation of precision landing performance for the baseline Apollo algorithm occurred as the result of two issues. First, the Upcontrol phase did not guide the vehicle to the desired exit conditions calculated by the Huntest phase. The control gains for the reference-following controller were likely designed with shorter target ranges in mind, and did not achieve the intended results for the longest target ranges. Second, the exit conditions calculated by Huntest were inaccurate due to an outdated assumption. Since the baseline Apollo algorithm was designed for target ranges of less than 4,600 km, the Kepler phase would always be short enough to ignore the effects of accumulated drag in the Kepler phase when calculating the exit conditions. For the much-longer target ranges intended for the CEV, this assumption is no longer valid. These two issues combined to cause severe undershoot in the longest target ranges.

IV. Results: Enhanced Guidance Algorithm

A. Enhanced Algorithm Description

The issues causing degradation in precision landing performance for long target ranges using the baseline Apollo algorithm were resolved by implementing three enhancements to the algorithm. First, the Upcontrol and Kepler phases were replaced with a numeric predictor-corrector (NPC) algorithm, which targets the second entry conditions rather than the atmospheric exit conditions. This change in the guidance phase logic is reflected in Fig. 7. The NPC algorithm used for this purpose, PredGuid, is an aerocapture NPC guidance algorithm developed for the Aero-assist Flight Experiment (AFE). The PredGuid algorithm is described in Ref. 8. An analytic predictor-corrector option was investigated but rejected due to the lack of a suitable closed-form expression to describe the entire skip trajectory.

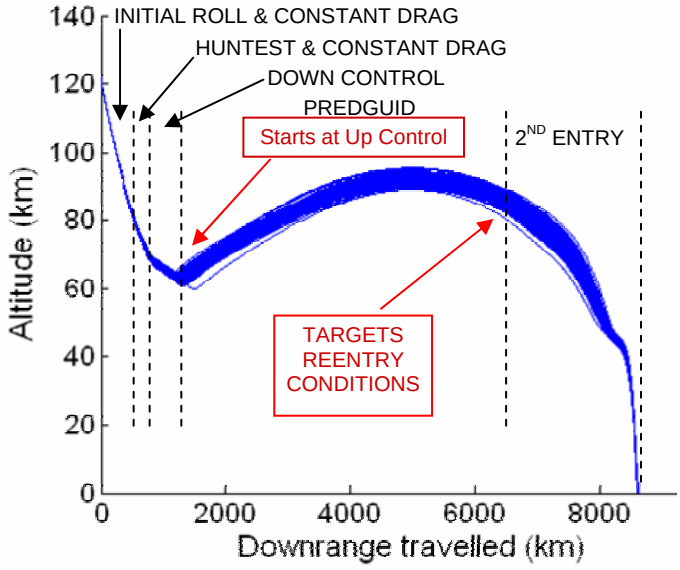

Fig. 7 Enhanced PredGuid Algorithm.

Next, the Final phase reference trajectory was redefined and extended to re-center it with respect to the CEV's range capability, since the CEV has different vehicle characteristics than the Apollo Command Module. Finally, the Final phase range estimation method used by the Huntest and PredGuid phases was updated to enable the new Final phase reference trajectory to support a wider spread of target ranges. More detail about the enhancements made to the algorithm is available in Ref. 9.

The effects of modulating the start time of the PredGuid phase was also investigated. A comparison was made between starting the PredGuid phase at the beginning of the Upcontrol Phase (as described above) and starting the PredGuid phase at the beginning of the Downcontrol phase. The difference in these two approaches resulted in different trajectory shaping. Starting the PredGuid phase at the nominal time by replacing the Upcontrol and Kepler phases resulted in a lower-altitude, shallower skip trajectory. Starting the PredGuid phase earlier by also replacing the Downcontrol phase resulted in a higher-altitude, steeper lofting.

B. Enhanced Algorithm Results

The results presented below detail the entry footprint of the CM using the enhanced numerical predictor-corrector guidance algorithm with both high and low lofting. Figures 5-10 show the landed accuracy, in terms of miss distance, of the CM at various downrange and crossrange commands for a given FPA. Figures 11 and 12 show the footprint outlines for high and low lofts for several FPAs.

Fig. 8 shows the footprint for a low loft at a FPA of -5.635 deg. The CM achieves a maximum crossrange of approximately ±750 km. The minimum downrange is 2250 km and significant accuracy is lost when downranges greater than 10000 km are targeted. The footprint for a low loft at a FPA of -5.900 deg is shown in Fig. 9. The CM achieves a maximum crossrange of ±850 km, an increase of 100 km over the -5.635 deg case. The minimum downrange decreases to 2000 km from 2500 km in the -5.635 deg case. Significant accuracy is still lost when downranges greater than 10000 km are targeted. The footprint for a low loft at a FPA of -6.100 deg is nearly identical to that of the -5.900 deg case (Fig. 10). Of note is the much larger red region starting at 11000 km, indicating a deterioration of long-range performance with steepening FPA.

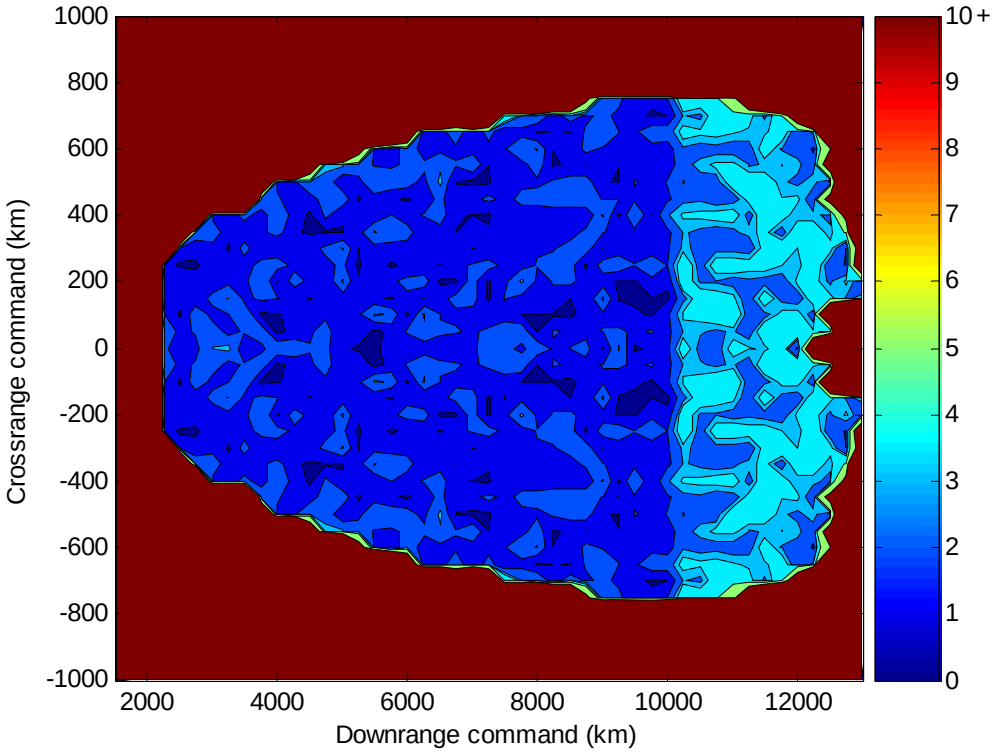

Fig. 8 Low Loft Miss Distance (km) With FPA = -5.635 deg.

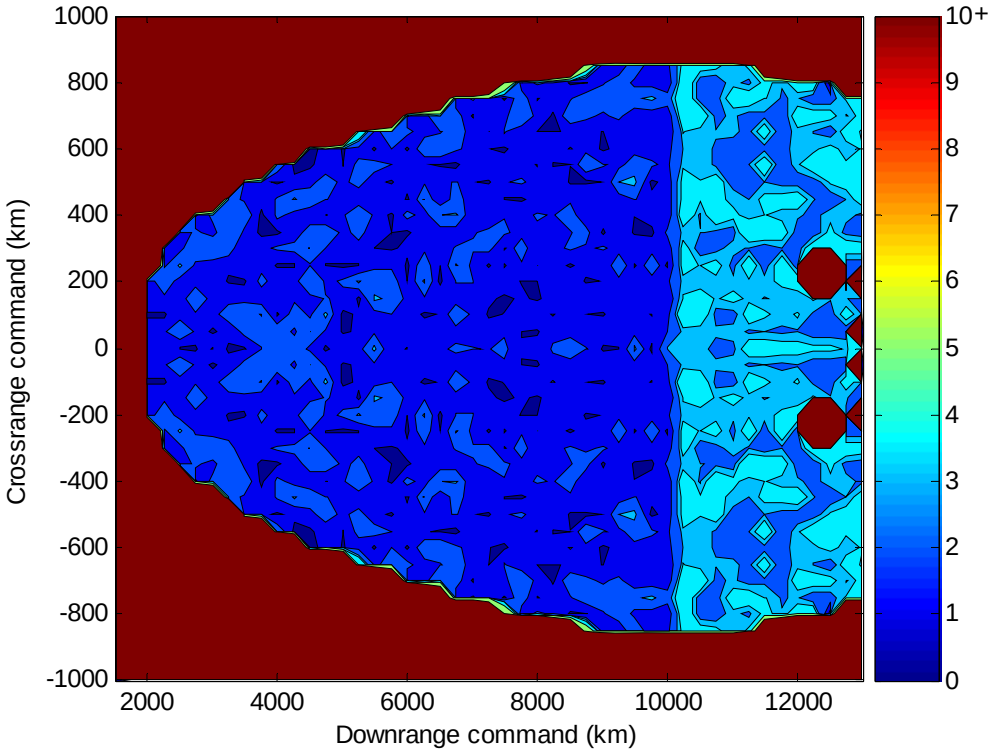

Fig. 9 Low Loft Miss Distance (km) With FPA = -5.900 deg.

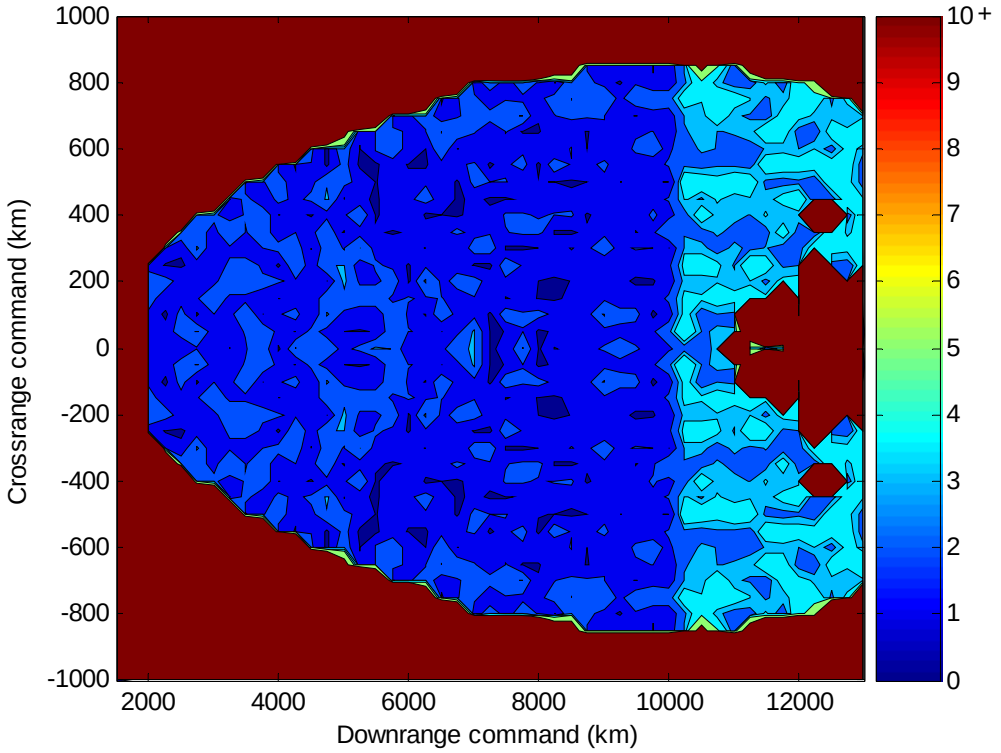

Fig. 10 Low Loft Miss Distance (km) With FPA = -6.100 deg.

Fig. 11 shows the footprint for a high loft at a FPA of -5.635 deg. The CM achieves a maximum crossrange of approximately ±900 km, a 150 km increase over the low loft case. The minimum downrange is 2250 km and the maximum downrange is 11250 km. No accuracy is lost between 10000 km and 11250 km as in the low loft case. The footprint for a high loft at a FPA of -5.900 deg is slightly better (Fig. 12). The CM achieves a maximum crossrange of ±950 km. The minimum downrange is 2000 km and the maximum downrange is 11000 km, slightly less than the -5.635 deg case. Of particular note are two regions of inaccuracy near 3000 km downrange. Fig. 13 shows the footprint for a high loft at a FPA of -6.100 deg. The CM achieves a maximum crossrange of ±900 km. Downrange performance is similar to the -5.900 deg case. The two inaccurate regions near 3000 km downrange have disappeared at this FPA.

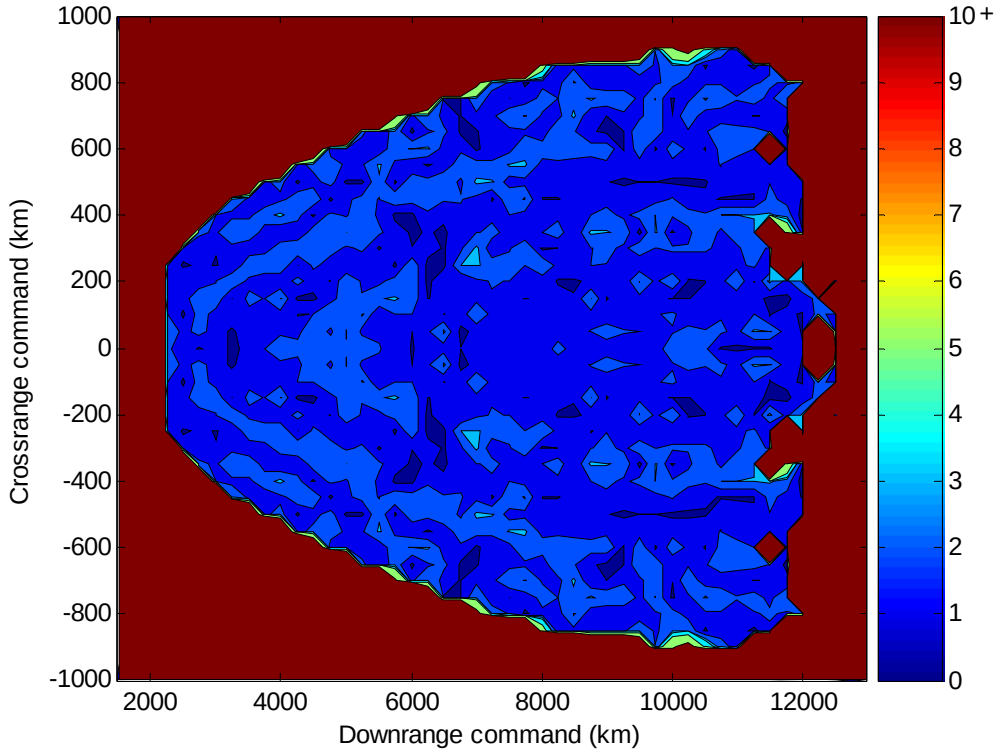

Fig. 11 High Loft Miss Distance (km) With FPA = -5.635 deg.

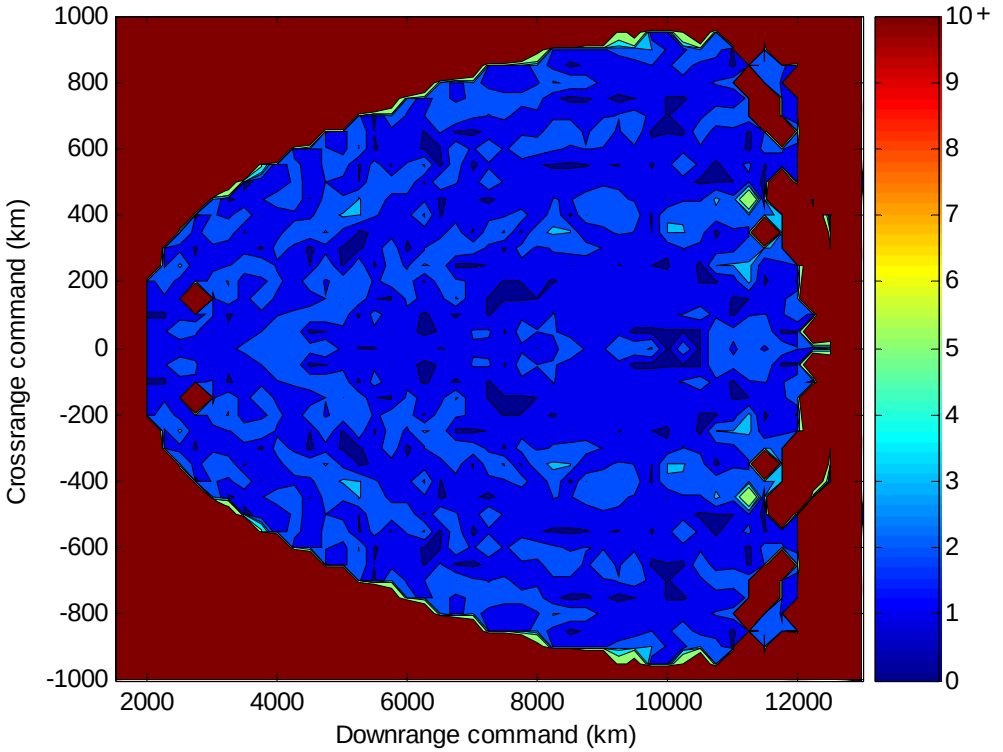

Fig. 12 High Loft Miss Distance (km) With FPA = -5.900 deg.

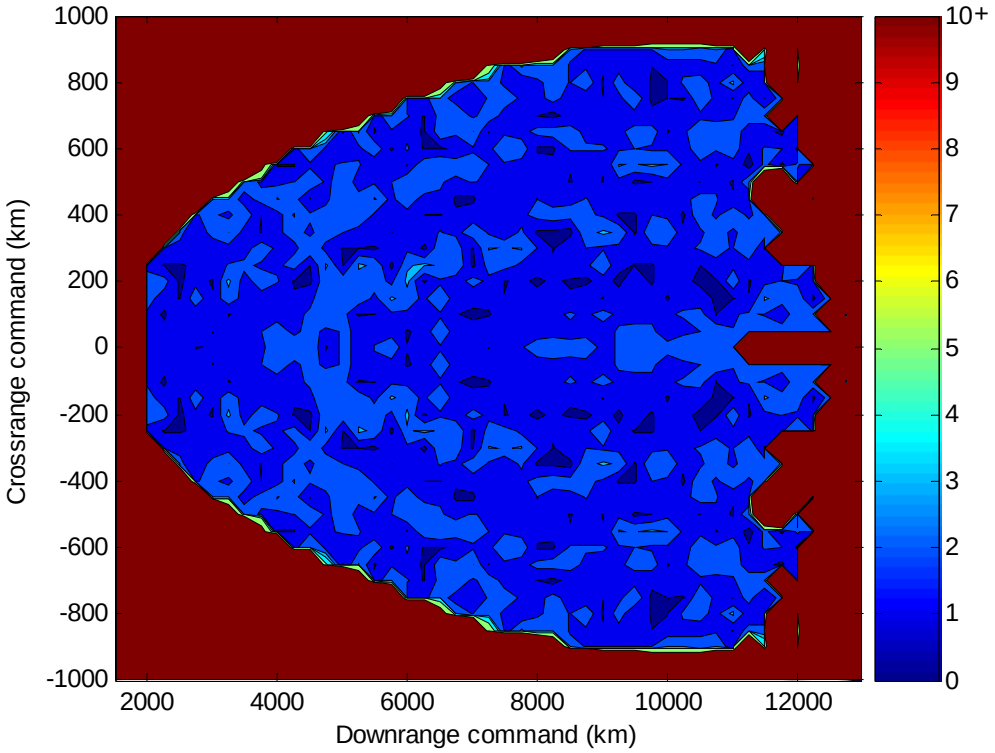

Fig. 13 High Loft Miss Distance (km) With FPA = -6.100 deg.

Fig. 14 and Fig. 15 show the footprints for low and high loft trajectories, respectively, at three FPAs. The footprint outlines correspond to miss distances of 3.5 km or less. As shown before, -5.900 deg and -6.100 deg provide similar performance, while -5.635 deg is slightly less capable. All trajectories begin to lose accuracy beyond 10000 km. As in the low loft cases, the performance of the high loft -5.900 deg and -6.100 deg cases is similar, with the exception of the two inaccurate regions in the -5.900 deg case near 3000 km downrange. The -5.635 deg case is slightly less capable in minimum downrange and maximum crossrange, but slightly more capable in maximum downrange, providing capability to 11250 km.

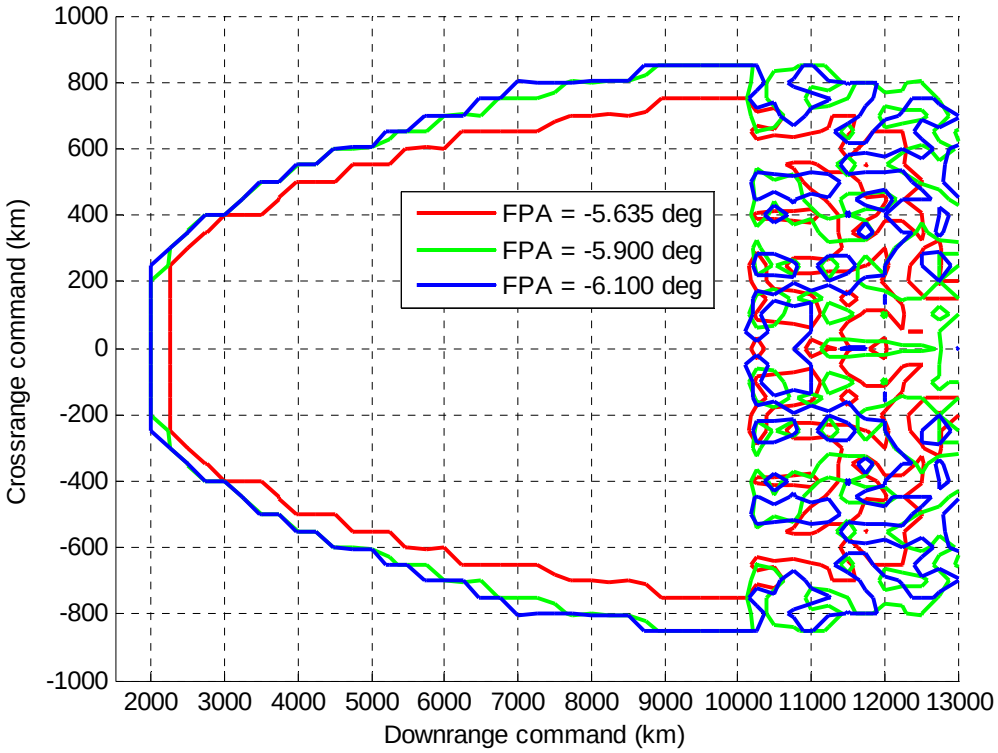

Fig. 14 Low Loft Footprints for Several FPAs, Miss Distance < 3.5 km.

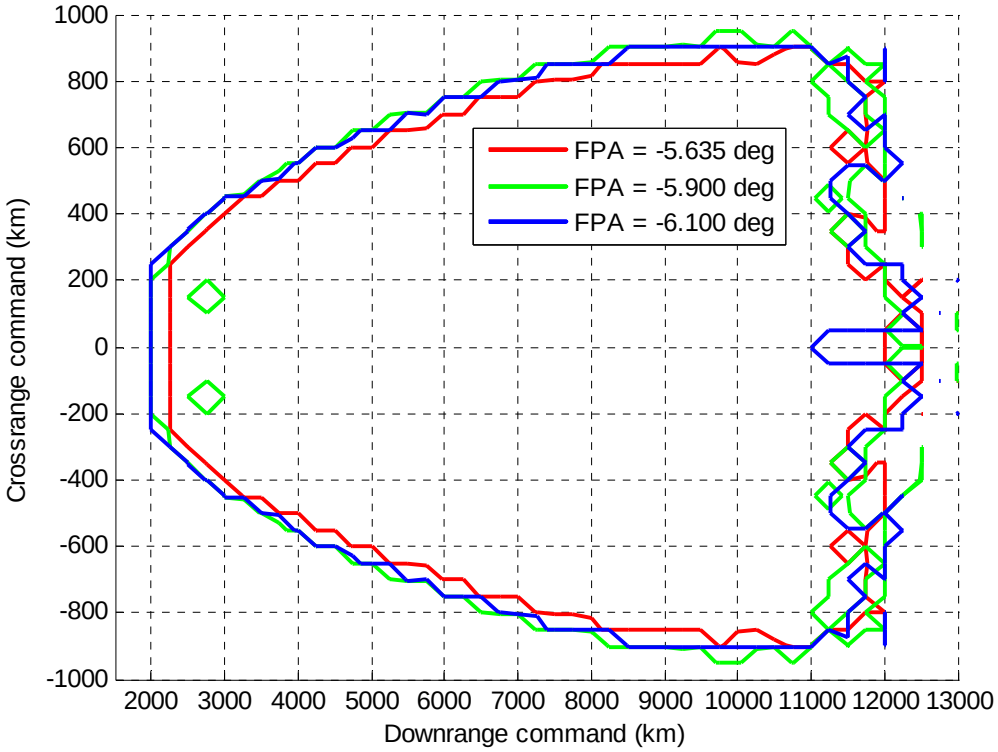

Fig. 15 High Loft Footprints for Several FPAs, Miss Distance < 3.5 km.

These data show that with the inclusion of the enhanced guidance algorithm, range performance is consistent over a large downrange and crossrange area. The shapes of the footprints are consistent with previous work performed with the Apollo CM. Over a range of FPAs, a crossrange of ±900 km is easily achievable with reasonable accuracy, while a downrange of 11000+ km is easily within the vehicle's capability. Table 4 provides a summary of the range performance data.

Table 4. Guided Range Performance Summary.

FPA	Minimum Downrange	Maximum Downrange	Maximum Crossrange
Baseline Algorithm			
-5.635 deg	2250 km	7000 km	±700 km
-5.900 deg	2000 km	7000 km	±700 km
-6.100 deg	2000 km	7500 km	±750 km
Low Loft Enhanced Algorithm			
-5.635 deg	2250 km	10000 km	±750 km
-5.900 deg	2000 km	10000 km	±850 km
-6.100 deg	2000 km	10000 km	±850 km
High Loft Enhanced Algorithm			
-5.635 deg	2250 km	11000 km	±900 km
-5.900 deg	2000 km	11000 km	±950 km
-6.100 deg	2000 km	11000 km	±900 km

As shown in Table 4, there is no significant change in landing accuracy within the range of FPAs examined. Miss distances of the CM remain within 3.5 km for low loft trajectories with downranges less than 10000 km. Miss distances of the CM remain within 3.5 km for high loft trajectories with downranges less than 11000 km, with the exception of two regions near 3000 km downrange at an FPA of -5.900 deg. It should be noted that these analyses include no uncertainty.

At steeper FPAs with a low loft trajectory, the maximum crossrange capability is increased slightly and the minimum downrange is decreased, both desirable effects. High loft trajectories exhibit similar minimum downrange performance with increased maximum crossranges. While the minimum downrange capability is better for steeper FPAs with high lofting, no clear advantage exists in crossrange performance for steep or shallow FPAs. It should be noted that a compromise between the high and low loft guidance algorithms could be implemented and that such an implementation would further decrease footprint dependence on FPA.

V. Conclusion

The CEV CM achieves significant capability footprint improvements over the baseline algorithm with use of the enhanced predictor-corrector entry guidance algorithm. With this algorithm, the CM can robustly achieve a maximum crossrange of ±900 km, a maximum downrange of 10000 km, and a minimum downrange of 2000 km while maintaining a landed accuracy within 3.5 km of the target. In addition, the CM footprint is largely independent of flight path angle at atmospheric interface.

Acknowledgments

This study was conducted with funding from the Charles Stark Draper Laboratory. The authors wish to acknowledge Steve Paschall (Charles Stark Draper Laboratory) for his work in developing the simulation used in this study.

References

[1] The White House Website Presidential News and Speeches, "President Bush Announces New Vision for Space Exploration Program," URL: http://www.whitehouse.gov/news/releases/2004/01/20040114-3.html, 26 October 2005.

[2] "Exploration Systems Architecture Study Final Report," NASA TM-2005-214062, November 2005.

[3] "NASA Solicitation: Conceptual Design of an Air Bag Landing Attenuation System for the Crew Exploration Vehicle." Langley Research Center Press Release, Dec. 14, 2005.
[4] Graves, Claude A., Harpold, Jon C., "Reentry Targeting Philosophy and Flight Results from Apollo 10 and 11," MSC 70-FM-48, March 1970.
[5] Tigges, M. et al. "Earth Land-Landing Analysis for the First Lunar Outpost Mission: Apollo Configuration," NASA JSC-25895, June 1992.
[6] Putnam, Z. R. et al. "Entry System Options for Human Return from the Moon and Mars," AIAA 2005-5915, AIAA Atmospheric Flight Mechanics Conference, San Francisco, CA, August 2005.
[7] Morth, R., "Reentry Guidance for Apollo," MIT/IL R-532 Vol. I, 1966.
[8] DiCarlo, J.L., *Aerocapture Guidance Methods for High Energy Trajectories.* S.M. Thesis, Department of Aeronautics and Astronautics, MIT, June 2003.
[9] Bairstow, S.H., *Reentry Guidance with Extended Range Capability for Low L/D Spacecraft.* S.M. Thesis, Department of Aeronautics and Astronautics, MIT, Feb. 2006.